Multipath model improvement for automotive radar application

Locatelli, Antonin; Alvarez-Perez, Jose Luis; Yarovoy, Alexander

DOI
10.23919/EuCAP60739.2024.10501729

Publication date
2024

Document Version
Final published version

Published in
Proceedings of the 2024 18th European Conference on Antennas and Propagation (EuCAP)

Multipath model improvement for automotive radar application

Antonin Locatelli*, Jose Luis Alvarez-Perez†, Alexander Yarovoy‡,
*ENAC, EMA research group, Toulouse, France, antonin.locatelli@alumni.enac.fr
†Polythechnic School, University of Alcala, Signal Theory and Communications, Madrid, Spain, joseluis.alvarez@uah.es
‡TU Delft, Microwave Sensing, Signals and Systems, Delft, The Netherland, A.Yarovoy@tudelft.nl

***Abstract*—Multi-path propagation over asphalt road surfaces at automotive radar frequencies is studied. A new expression for the reflection coefficient from asphalt which takes into account asphalt surface roughness is proposed. The classic two-ray method to take into account the multi-path is improved using antenna radiation patterns and the antenna tilt. A new method to estimate elevation of a reflector above road surface based on reflectivity variations is proposed.**

***Index Terms*—antennas, electromagnetic wave, propagation, multipath, rough surface, target reflectivity fluctuations.**

I. Introduction

In automotive radar application [1], multi-path propagation due to reflection from road surface plays an important role. Typically, the road surface is considered to be flat, leading to only specular (forward) reflection. In reality, the surface roughness and internal structure of asphalt results in scattering in all directions.

Concerning the multipath, this well-known phenomenon is responsible for reflected signal fluctuations and fading due to destructive interferences from received waves. If the attenuated signal decreases and becomes lower than the sensitivity of the receiver, the target could disappear.

The purpose of this study is firstly to correct a road reflection forward-scattering coefficient, by taking correctly into account impact of the surface roughness. In the previous studies [2][3] only the coherent reflection has been considered. Secondly, to improve the initial multipath model by taking into account the tilt and the radiation pattern of the antenna and also the area stricken by the electromagnetic wave, which is different with respect to the situation. Influence of a reflector height above the road on fluctuations of the propagation loss due to multi-path is also studied and a novel method to estimate the reflector height from target return fluctuations is proposed.

In Section II, propagation model is described, in Section III, the chosen form of the road reflection coefficient is explained. The multipath model and its improvements are clarified in Section IV. Section V presents results of numerical analysis and, finally, Section VI concludes this paper.

II. Generic electomagnetic model

A. Relation between field amplitude and power

In far field, the electromagnetic wave created by an antenna could be written, in spherical coordinates as $\mathbf{E}(r,\theta,\phi) = \mathbf{e}_0(\theta,\phi)\frac{e^{-jkr}}{r}$, where k is the wave number. Then, the radiant intensity could be defined as

$$U(\theta,\phi) = \frac{\mathrm{d}P}{\mathrm{d}\Omega} = \frac{\|\mathbf{E}\|^2}{2\zeta}r^2 = \frac{\|\mathbf{e}_0\|^2}{2\zeta}, \tag{1}$$

where P is the power, Ω the solid angle and ζ the media impedance. Furthermore, let's remind the definition of the gain G of an antenna,

$$G = \frac{U}{U_{iso}} = \frac{4\pi}{P_f}U, \tag{2}$$

where iso stand for isotropic and P_f if the power supplied to the antenna.

Finally, combining (1) and (2),

$$\|\mathbf{e}_0\|^2 = \frac{\zeta G P_f}{2\pi}. \tag{3}$$

B. Relation between reflection coefficient and radar cross section

Let's consider the diffraction of a wave by a random object. This object has a reflection coefficient R and a radar cross section σ and situated at the distance δ_1 from transmitter and distance δ_2 from the receiver. In order to linked these two quantities, the surface power density arriving in the receiver position A is calculated by two different ways.

Firstly, considering object as extended surface with the reflection coefficient R the incident field at the receiver could be written, thanks to geometrical optics, as $\mathbf{E}_A = \mathbf{e}_0 R\frac{e^{-jk\delta}}{\delta}$, where $\mathbf{e}_0$ is defined above and δ=δ_1+δ_2, the total distance. Then, the surface power density could be written

$$P_{s_A}^{(1)} = \frac{\|\mathbf{E}_A\|^2}{2\zeta} = \frac{\|\mathbf{e}_0\|^2|R|^2}{2\zeta\delta^2}. \tag{4}$$

Secondly, the radar equation could be used to express the power in another form, as

$$P_{s_A}^{(2)} = \frac{P_f G}{4\pi\delta_1^2}\sigma\frac{1}{4\pi\delta_2^2}. \tag{5}$$

Finally, combining (3), (4) and (5), the relation becomes

$$\sigma = 4\pi|R|^2\frac{\delta_1^2\delta_2^2}{(\delta_1+\delta_2)^2}. \tag{6}$$

III. Reflection coefficient

In this part, the surface roughness is assumed to be normally distributed and characterised by its root-mean-square height s and correlation length l. Its reflection coefficient is studied.

A. Theory

As it will be seen in Section IV only the specular component is studied. As the reflection happened on a rough surface, two components of the reflected field have to be taken into account: the coherent and the incoherent part [4]. Correspondingly, the total reflection coefficient has also two components. For the coherent part, the usual modified Fresnel's coefficients [2] are used. For the incoherent part, the IEM2Mc model is used [5]. This latter model is an improvement on the old IEM2M model.

More precisely, the normalised radar cross section $(\sigma^0)^S_{pq}$, where S means *single-scattering* and qp denotes the polarization is calculated using

$$(\sigma^0)^S_{pq} = \frac{1}{2}k^2 e^{-s^2(k_{sz}-k_z)^2} \times \sum_{n=1}^{\infty} \frac{s^{2n}}{n!} |\mathcal{I}^{(n)}_{qp}|^2 W^{(n)}_1(k_{sx}-k_x, k_{sy}-k_y), \quad (7)$$

where $\mathbf{k}=(k_x, k_y, k_z)$ is the incident wavenumber, $k=|\mathbf{k}|$, $\mathbf{k}_s = (k_{sx}, k_{sy}, k_{sz})$ is the scattered wavenumber, s is the standard deviation of the surface, $W^{(n)}_1$ is the Fourier transform of the n-th power of the surface height distribution and $\mathcal{I}^{(n)}_{qp}$ is a function detailed in [5].

However, this model gives only the amplitude. Then, the phase Φ is a random variable following a uniform law ($\Phi \sim \mathbb{U}[0, 2\pi]$) [6]. The reflection coefficient is then written

$$R = R_{fres}\rho_s + |R_{iem2mc}|e^{j\Phi}, \quad (8)$$

where k is the wavenumber, R_{fres} is the Fresnel's coefficient, $\rho_s = e^{-2k^2 s^2 \cos^2\theta}$ [3] and R_{iem2mc}, the value of the reflection coefficient which is computed using the normalized bistatic coefficient σ^0_{iem2mc} and (6).

B. Numerical simulation

Fig. 1 shows the amplitude of three different reflection coefficients for an horizontal polarization and a rough surface with respect to the incidence angle θ. The normalized RMS height is ks=0.8, the normalized correlation length is kl=0.3 and the asphalt relative permittivity is ϵ_r=3.3, this three parameters are assumed to be constant when the car is moving. The reflection coefficients are the Fresnel one, the modified Fresnel one and the final one defined by (8). In the computation, there are no average. That is to say that only one value of R_{iem2mc} for each angle has been used. Furthermore, it is assumed here that $|R_{iem2mc}| = \sqrt{\sigma^0_{iem2mc}}$.

The attenuation of the modified Fresnel's due to the roughness is less present for grazing angles (Fig. 1), due to the dependence of $\cos\theta$ in ρ_s. Then, the final coefficient follows the value of the modified Fresnel's coefficient, the fluctuation due to the scattered part decreases when θ increases, which is due to the known result that scattered component amplitude decreases when the incident angle increases. If an average had been calculated, the final coefficient would have been more similar to the yellow curve.

Concerning the phase, not visible here due to the length limitation, the classic and modified Fresnel's coefficient have always a phase of 180° (which simply mean that the coefficients are negative) whereas the final coefficient shows some fluctuation but always around 180°.

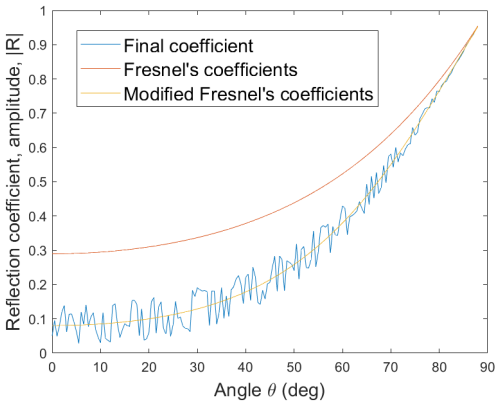

Fig. 1. Amplitude of three different types of reflection coefficients as functions of the incident angle.

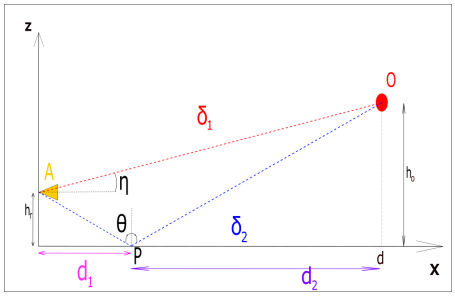

Fig. 2. Representation of the two ray multipath model.

IV. Multipath Model

In this section, a model for multipath phenomenon including surface roughness is presented. All notations for lengths or angles are visible in the Fig. 2. Furthermore R stands for the reflection coefficient (in this part, its value has no importance). Furthermore, as the work frequency is chosen at 77 GHz, the loss due to the atmosphere is neglected.

A. The original two-ray model

The equations of multipath problem are well known [4]. Then, in this paper, a return trip is considered. The wave is created by the antenna A, it takes the two path δ_1 and δ_2, it is reflects by the object O and returns to A using two paths. If P_r is the return power and P_f is the provided power, the equation is

$$\frac{P_r}{P_f} = \frac{\sigma_o}{(4\pi)^3}\frac{G^2\lambda^2}{\delta_1^4}\left|1 + R' e^{-jk\Delta\delta}\right|^4, \quad (9)$$

where σ_o is the radar cross section of O, $\Delta\delta$=δ_2-δ_1, k is the wave number, λ the wavelength, G the antenna gain and R'=$\frac{\delta_1}{\delta_2}R$.

B. The improvements

Even if the previous result gives good approximation, this study would like to go further and to take into account three enhancements : a radiation pattern, a tilt and an area stricken by the wave.

Inclusion of the radiation pattern: The gain is only considered in the (xOz) plane, then the radiation pattern is taken into account by writing the gain with respect to the angle, hence $G(\eta)$. This radiation pattern has to be taken into account at the transmission and at the reception. It is assumed here that the maximum gain is for η = 0°, that is to say at the horizontal. In the next calculation, the electric field is supposed to be scalar.

Let's begin to write the field from the antenna as $E(r,\eta) = e_0(\eta)\frac{e^{-jkr}}{r}$, with $e_0(\eta) = \sqrt{\frac{\zeta}{2\pi}G(\eta)P_f}$. Then, by summing the field from the two paths, the electric field arriving in O can be written

$$E(O) = e_0(\eta_1)\frac{e^{-jk\delta_1}}{\delta_1}\left(1 + \frac{e_0(\eta_2)}{e_0(\eta_1)}\frac{\delta_1}{\delta_2}Re^{-jk\Delta\delta}\right). \quad (10)$$

Then, the power returned by O is written $P_r(O) = \sigma_o\ \frac{|E(O)|^2}{2\zeta}$ and the return field from O is written

$$E^{(ret)}(r) = e_0^{(ret)}\frac{e^{-jkr}}{r}, \quad (11)$$

with $e_0^{(ret)}$=$\sqrt{\frac{\zeta P_r(O)}{2\pi}}$.

Now, both the antenna gain and interferences have to be taken into account at A. In order to do this, the gain is put into the expression of the field and the antenna is then supposed isotropic. The only thing to do is to consider an $effective$ value of e_0 namely $e_{0,eff}$ such as $e_{0,eff} = \sqrt{G}e_0$.

Thus, the field arriving in A by both path could be written

$$E^{(ret)}(A) = e_0^{ret}\frac{e^{-jk\delta_1}}{\delta_1}\sqrt{G(\eta_1)}\left[1 + R''e^{-jk\Delta\delta}\right], \quad (12)$$

where R''=$R'\sqrt{\frac{G(\eta_2)}{G(\eta_1)}}$ and η_1 and η_2 are the elevation angles of the direct and the multipath, respectively.

Finally, the receive power could be written similarly to (9) as

$$\frac{P_r}{P_f} = \frac{\sigma_o}{(4\pi)^3}\frac{G(\eta_1)^2\lambda^2}{\delta_1^4}\left|1 + R''e^{-jk\Delta\delta}\right|^4. \quad (13)$$

Inclusion of an antenna tilt: In order to take into account an antenna tilt, that is to say a maximum of radiation which is not for η=0°, the only thing to do is change η to $\eta - \eta_{max}$, where η_{max} is the value of the elevation where the power is the highest.

Inclusion of the area: The IEM2Mc model program used for this study gives the normalized forward-scattering coefficient σ^0. In order to get the real forward-scattering coefficient σ, σ^0 has to be multiplied by the area stricken by the wave A. The criteria "-3dB" is used to delimited the area, that is to say the incident surface power density is calculated on the ground, the maximum P_{max} is found and each point on the ground where surface power density is superior to $\frac{P_{max}}{2}$ is taken into account in the calculation of the area.

C. The final multipath model

For the following section, the formula will be (13). The value of R is given using (8). By taken into account some geometrical relations (see Fig. 2), we get

$$|R_{iem2mc}| = \sqrt{\frac{A\sigma^0}{4\pi}}\frac{h_r + h_o}{h_r h_o}|\cos\theta|. \quad (14)$$

V. Numerical analysis

In this part, the previous model and (13) is applied and some plots are shown to represent and compare the improved model with respect to the classical model.

For the upcoming simulation, the following parameters have been fixed: the frequency f = 77 GHz, h_r = 30 cm and h_0 = 1.7 m. Given that the far-field distance is approximately 5 meters, assuming the antenna size is around a dozen centimeters, $d \in [5, 100](m)$. The radar cross section of the object is assumed to be constant with respect to the angle of arrival, σ_o = 1 m^2. This assumption is significant and could be further refined in subsequent studies. The surface reflection coefficient is determined by averaging 25 random surface realizations. Lastly, all values for power, gain, and threshold are derived from the Type A radar specifications recommended by the ITU [7].

In Figures 3a and 3b, we explore the impact of surface roughness. In both figures, the blue curve denotes the scenario without multipath ($R = 0$), while the yellow curve depicts the scenario without scattering, displaying only the coherent part. The similarity of these curves is anticipated due to several factors. First, only the surface parameters vary between the two plots, resulting in an unchanged no-multipath case. Second, the attenuation factor ρ_s depends solely on the constant value of ks. Third, the influence of the relative permittivity ε_r on Fresnel's coefficients is minimal, particularly at grazing angles, as observed here. The noticeable bump in both figures arises from the antenna gain; its differing shapes correspond to the gain's varied expression relative to the elevation angle, as described in [7]. This effect manifests differently from 5m to around 20m, where the logarithmic part of the gain is evident, and beyond 20m, where the square part becomes prominent. As the distance increases, the incident angle on the surface also increases, thereby diminishing oscillations near 5m due to the higher ρ_s factor at lower incident angles.

In Fig. 3b, in contrast to Fig. 3a, the incoherent part is distinctly visible. The signal exhibits faster and more erratic oscillations, attributable to the random phase. The greater the distance, the less pronounced the incoherent part becomes. This aligns with the observations in Fig. 1 that the reflection coefficient decreases with increasing incident angle. The more noticeable incoherent part in Fig. 3b is due to the longer correlation length. A higher correlation length, compared to the surface slope $\left(\frac{s}{l}\right)$, results in scattering that is more concentrated in the specular direction, thereby increasing the incoherent reflection coefficient.

In Fig. 4, the normalized received power is depicted for varying antenna tilt angles η_{max}. When the antenna points

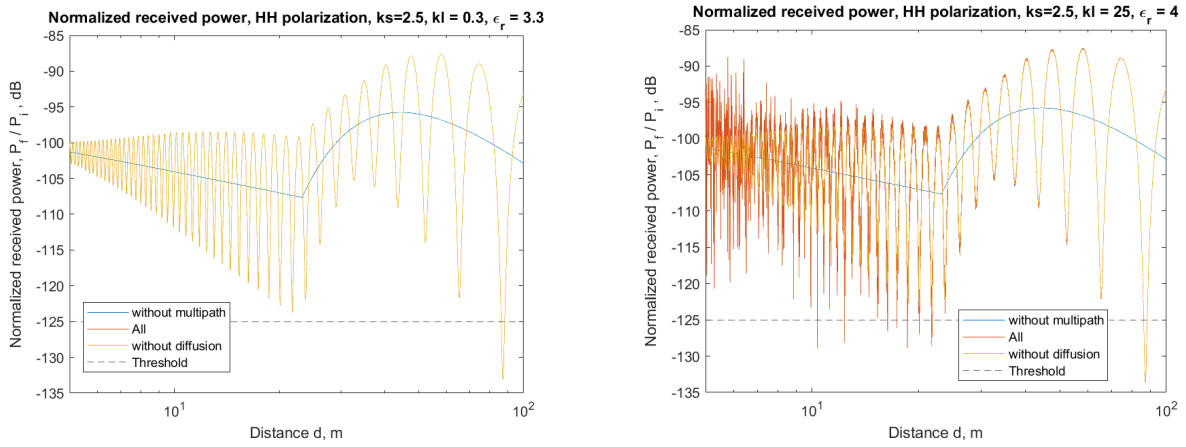

(a) Low presence of the incoherent power.

(b) High presence of the incoherent power.

Fig. 3. Representation shows the normalized received power as a function of distance for various rough surface parameters, with $\eta_{max} = 0°$. The threshold indicates the receiver's normalized sensitivity[7]. In the left figure, yellow and orange curves coincide.

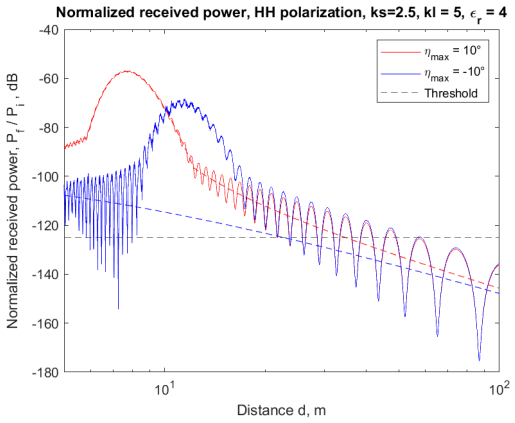

Fig. 4. Representation of the normalized receive power with respect to the distance, for two different values of η_{max}. The threshold represent the normalized sensitivity of the receiver, from [7]. The dotted line represent the power without multipath (just the direct path).

above the road ($\eta_{max} > 0$), the bump appears in both scenarios, with and without multipath. This occurrence is expected, as in both cases, the direct path traverses the antenna's most amplified direction. Conversely, when the antenna points towards the ground ($\eta_{max} < 0$), only the indirect path aligns with the most amplified direction, explaining the absence of a bump in the no-multipath scenario.

An interesting observation in Fig. 4 is the significant oscillation of the blue curves for distances $d < 10m$. Upon examining the reflection coefficient over distance (not shown due to paper length constraints), it appears that its absolute value approaches 1 at these distances. Analyzing (13) reveals that if $R'' \sim 1$, the received power $P_f \to 0$ (or $-\infty$ in dB).

As the distance increases, the normalized received powers for both cases are similar. Over longer distances, free-space loss predominates, diminishing the differences in gain. Additionally, both angles η_1 and η_2 tend towards 0°. Since the gain is symmetric and both η_{max} values are equally absolute (10°), the gain becomes similar for both cases.

Notably, the oscillations atop the hump are more pronounced when the antenna tilts towards the ground compared to when it points towards the object. This aligns logically with the factor $\sqrt{\frac{G(\eta_2)}{G(\eta_1)}}$: the closer $|R''|$ is to 1, the greater the oscillation. Furthermore, since $|\eta_2| \geq |\eta_1|$ and considering the η_{max} value, the aforementioned factor is larger when $\eta_{max} < 0$.

The issue of multipath, as discussed in this paper, is also addressed by other researchers [8] [9]. While their models of multipath differ, their findings exhibit some similarities to those depicted in Fig. 3 and Fig. 4.

Moreover, as Mizutani et al. [10] have demonstrated, altering the height of the radar antenna or the object significantly affects the strength of the received signal. In Fig. 5, we plot the normalized received power against the distance d for different object heights h_o, leading to several notable observations.

Firstly, the rapid fluctuations, attributed to the statistical phase value of the incoherent part of the reflection coefficient (8), diminish as distance d increases. This aligns logically with the decrease in the absolute value of the incoherent normalized forward-scattering coefficient as the incident angle θ increases, as illustrated in Fig. 1. Secondly, a higher object height (h_o) leads to faster oscillations. This is understandable since the oscillations stem from the term $k\Delta\delta$ in (13). Given that k is constant, these oscillations originate from $\Delta\delta$, which approximately equals $\frac{2h_r h_o}{d}$; thus, a larger h_o results in greater variations in $\Delta\delta$ and subsequently more pronounced oscillations with increasing d. Thirdly, the notable power increase in the violet and green curves, appearing as a bump, is attributed to the paths entering the main beam of the radar antenna at a certain distance. Fourthly, across all curves, the amplitude of oscillations grows with distance. This is due to two factors: the decreasing difference in free-space loss between the two paths and the increasing similarity of η_1 and η_2. These factors make the powers of the direct and indirect

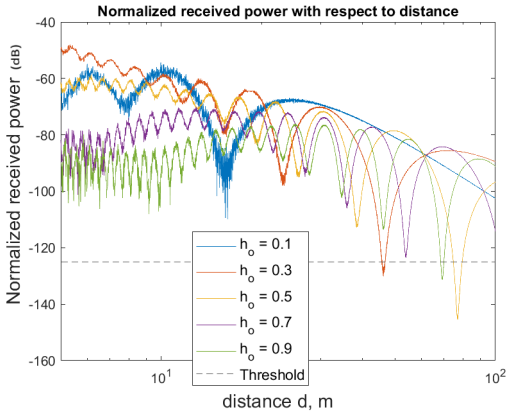

Fig. 5. Normalized received power in dB against distance d for varying h_o values. The parameters are set as follows: $ks = 2.5$, $kl = 25$, $\varepsilon_r = 4$, with horizontal polarization, $\sigma_o = 1$, and the reflection coefficient averaged over 25 instances.

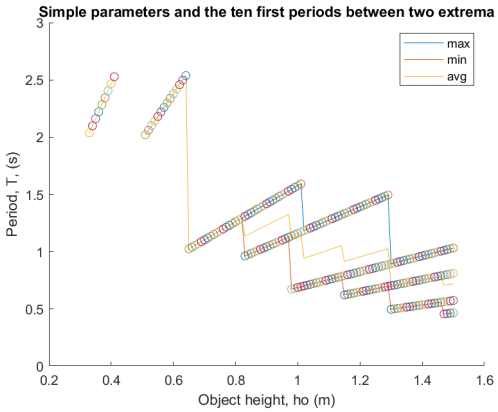

Fig. 6. Periods between extrema, as well as the maximum, minimum, and average values, for multiple circles representing the same object height. In this scenario, the object is located between 50 and 100 meters from the car, with the car traveling at a speed of 50 kilometers per hour.

paths more comparable, leading to stronger interferences and larger oscillations. Finally, the closer h_0 is to h_r, the higher the power. This is simply because, in such cases, the angle η of the direct path is close to zero, resulting in maximum gain.

In the final section, we explore a method, as analyzed in [11], to detect the height of a reflector target using fluctuations caused by multipath. Consider a car moving at a certain speed and an object with a specific height h_o. It's feasible to chart the normalized received power over time, and then calculate the duration between two extremes. Given that a radar gauges target range, selecting a distance interval (e.g., between 50 and 100 meters) is possible. In Fig. 6, circles denote oscillation periods for a given target height. When multiple h_o values correlate with different circles, we calculate and depict the minimum, maximum, and average of these values with solid lines.

This reveals intriguing insights. First, a higher object height correlates with a greater number of periods, a conclusion consistent with previous findings. Second, using just one of the functions (min, max, avg) alone doesn't allow for an unambiguous height association due to their non-injective nature. However, employing the triplet (min, max, avg) establishes a bijective relationship with the object height. Therefore, this triplet can be effectively used to estimate an object's height.

VI. Conclusion

A new deterministic model for the multipath in automotive context is proposed. The model takes into account scattering from rough road surface, the radiation pattern and the tilt of the antenna. Then, numerical analysis of the normalized received power, with respect to distance d for different surfaces, different kind of reflections, different antenna tilts and different object heights is performed. Finally, a method to estimate the height of the object using the fluctuation of the received power is given. The model proposed can be integrated in the frameworks of the automotive cruise control and more generally into the advanced driver-assistance system. However, it's crucial to note that the presence of other objects in the environment might impact the proposed model, and their influence should be considered in future studies.

Acknowledgment

The first author would particularly like to thank all people of the MS3 lab at Delft University of Technology who welcomed and helped him during fourteen marvellous weeks he spent on internship in the Netherlands. The financial support of Erasmus+ program to the first author is also appreciated.

References

[1] M. Schneider, "Automotive radar: Status and trends," in Proc. German Microwave Conf. (GeMiC), Ulm, Germany, Apr. 2005, pp. 144–147

[2] R. Schneider, D. Didascalou and W. Wiesbeck, "Impact of road surfaces on millimeter-wave propagation," in IEEE Transactions on Vehicular Technology, vol. 49, no. 4, pp. 1314-1320, July 2000, doi: 10.1109/25.875249.

[3] R. D. De Roo and F. T. Ulaby, "A modified physical optics model of the rough surface reflection coefficient," IEEE Antennas and Propagation Society International Symposium. 1996 Digest, Baltimore, MD, USA, 1996, pp. 1772-1775 vol.3, doi: 10.1109/APS.1996.549946.

[4] R. M. Narayanan, D. D. Cox, J. M. Ralston and M. R. Christian, "Millimeter-wave specular and diffuse multipath components of terrain," in IEEE Transactions on Antennas and Propagation, vol. 44, no. 5, pp. 627-, May 1996, doi: 10.1109/8.496248.

[5] J. L. Alvarez-Pérez, "The IEM2M rough-surface scattering model for complex-permittivity scattering media," Waves Random Complex Media, vol. 22, no. 2, pp. 207–233, May 2012.

[6] BECKMANN, Petr et SPIZZICHINO, Andre. "The scattering of electromagnetic waves from rough surfaces." Norwood, 1987.

[7] ITU-R M.2057-1, 2018,

[8] M. Buhren and B. Yang, "Extension of Automotive Radar Target List Simulation to consider further Physical Aspects," 2007 7th International Conference on ITS Telecommunications, Sophia Antipolis, France, 2007, pp. 1-6, doi: 10.1109/ITST.2007.4295847.

[9] H. -N. Wang, Y. -W. Huang and S. -J. Chung, "Spatial Diversity 24-GHz FMCW Radar With Ground Effect Compensation for Automotive Applications," in IEEE Transactions on Vehicular Technology, vol. 66, no. 2, pp. 965-973, Feb. 2017, doi: 10.1109/TVT.2016.2565608.

[10] K. Mizutani and R. Kohno, "Analysis of multipath fading due to two-ray fading and vertical fluctuation of the vehicles in ITS inter-vehicle communications," Proceedings. The IEEE 5th International Conference on Intelligent Transportation Systems, Singapore, 2002, pp. 318-323, doi: 10.1109/ITSC.2002.1041236.

[11] S. Kohnert, M. Vogt and R. Stolle, "FMCW Radar Height Estimation of Moving Vehicles by Analyzing Multipath Reflections," Proceedings. The 20th European Radar Conference, Germany, 2023 pp. 30-33.